GEOLOGIJA 68/2, 243-250, Ljubljana 2025
© Author(s) 2025. CC Atribution 4.0 License

https://doi.org/10.5474/geologija.2025.010
Article

Transmission electron microscopy analysis of shock veins in the meteorite Jesenice

Presevna elektronska mikroskopija udarnih žil v meteoritu Jesenice

Bojan AMBROŽIČ[1], Sašo ŠTURM[2,3] & Mirijam VRABEC[3*]

[1]Center of Excellence on Nanoscience and Nanotechnology – Nanocenter, Jamova c. 39, SI-1000 Ljubljana, Slovenia; e-mail: bojan.ambrozic@nanocenter.si
[2]Jožef Stefan Institute, Jamova c. 39, SI-1000 Ljubljana, Slovenia; e-mail: saso.sturm@ijs.si
[3*]Faculty for Natural Sciences and Engineering, Department for Geology, Aškerčeva cesta 12, SI-1000 Ljubljana, Slovenia; *corresponding author: mirijam.vrabec@ntf.uni-lj.si

Prejeto / Received 27. 8. 2021; Sprejeto / Accepted 9. 10. 2025; Objavljeno na spletu / Published online 10. 12. 2025

Key words: chondrite, shock stage, shock veins, metal-sulfide globules, tetrataenite, transmission electron microscopy
Ključne besede: hondrit, udarna metamorfoza, udarne žile, kovinsko-sulfidne globule, tetrataenit, presevna elektronska mikroskopija

Abstract

Meteorite Jesenice is a weakly (S3) shocked ordinary chondrite from Slovenia. The shock event was violent enough to cause localized partial melting of the meteorite and the formation of shock veins. Inside the shock veins, metal-sulfide globules were found, which provided evidence for a post-shock cooling rate of $2.2 \cdot 10^5$ Ks^{-1} – $7.4 \cdot 10^3$ Ks^{-1}. From the mineral paragenesis of the shock veins, shock pressure and peak shock temperature were deduced as 2.5–15 GPa and 1500–2150 °C, respectively. We provide evidence that shock veins were formed via a shear and friction mechanism. Furthermore, the confirmed presence of ordered FeNi metal (tetrataenite) found in the matrix indicates that the shock occurred in the parent body of the meteorite Jesenice.

Izvleček

Meteorit Jesenice je šibko udarno metamorfoziran (S3) navadni hondrit iz Slovenije. Udarni dogodek je bil dovolj silovit, da je povzročil delno taljenje meteorita in s tem nastanek udarnih žil. V udarnih žilah so bile najdene kovinsko-sulfidne globule, s katerimi smo določili hitrost ohlajanja na $2.2 \cdot 10^5$ K s^{-1} – $7.4 \cdot 10^3$ K s^{-1}. Iz mineralne združbe udarnih žil smo določili najvišji udarni tlak in najvišjo temperature na 2.5–15 GPa oz. 1500–2150 °C. Sklepamo, da je do nastanka žil prišlo z mehanizmom strižnega trenja. V meteoritu smo potrdili tudi obstoj minerala tetrataenita, kar nakazuje, da je do dogodka udarne metamorfoze prišlo znotraj starševskega telesa meteorita Jesenice.

Introduction

Meteorite Jesenice fell on April 9, 2009 on the Mežakla Plateau near the town of Jesenice as a spectacular fireball, frightening the residents (Bischoff et al., 2011). Three stones with a total mass of 3.67 kg were later recovered. Analyses carried out by Bischoff et al. (2011) showed that it is a weakly shocked ordinary (L6 S3) chondrite. The shock stage of the meteorite is a fundamental property because it reflects the intensity of impact processes that shaped the meteorite's parent body and provides essential information on solar system collisional evolution (Stoffler et al., 1992). There are several studies on shock veins and the effects of local melting in moderately and strongly shocked chondrites (Acosta-Maeda et al., 2013; Guo et al., 2020; Kong & Xie, 2003). However, local melting in weakly shocked chondrites has been poorly studied (Owocki & Muszyński, 2012; Xie et al., 2006). In the following paper, we study in detail the shock veins and the ordered FeNi phase (tetrataenite) in order to better understand the conditions of shock metamorphism in the weakly shocked meteorite Jesenice, specifically the mechanism of shock vein formation and the subsequent thermal history recorded by the preservation of tetrataenite.

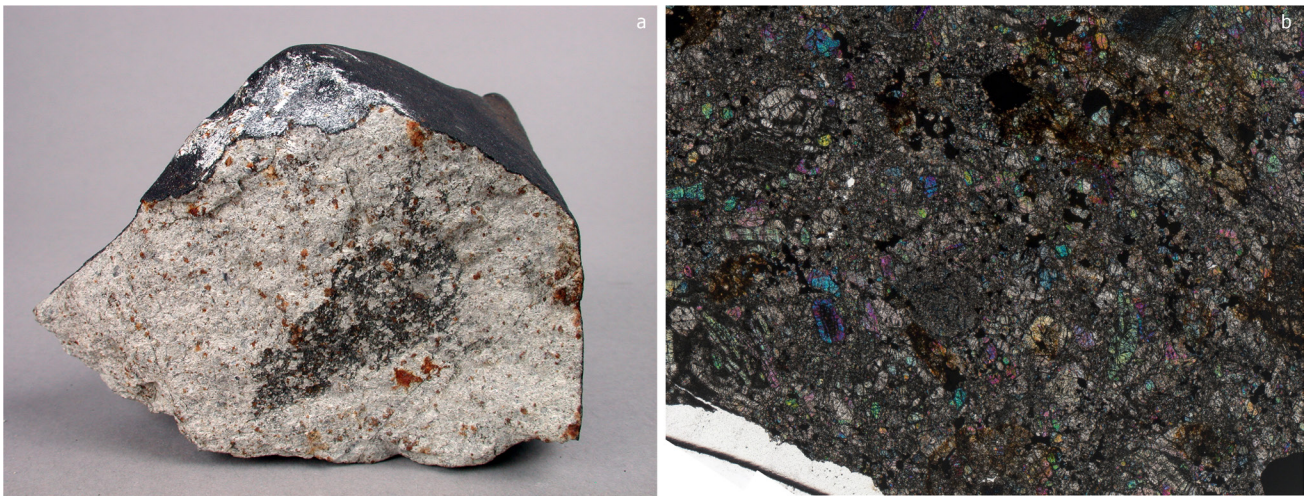

Fig. 1. Meteorite Jesenice, which fell on 9 April 2009 on the Mežakla Plateau: (a) hand specimen (photo: Miha Jeršek), and (b) polished thin section 1M.

Experimental section

Sample preparation

Polished thin sections, 30 μm thick, were prepared from the meteorite Jesenice (Fig. 1). For scanning electron microscope observations, the sections were coated with a 3 nm layer of amorphous carbon to ensure electrical conductivity.

Analytical methods

Polished thin sections were examined with a Zeiss Axio Z1-m optical microscope (Jožef Stefan Institute, Ljubljana) in transmitted and reflected light under crossed and parallel polarizers at magnifications 100–1000×.

Scanning electron microscopy (SEM) imaging was performed using JEOL JSM-5800, JEOL JSM-7600F, FEI Helios NanoLab 650, JEOL JIB-4601F, and JEOL JSM-840 at facilities in Slovenia (Jožef Stefan Institute, Nanocenter), Turkey (Sabanci University Nanotechnology Center), and Slovakia (SGIDS, Bratislava). Images were collected using backscattered electrons (BSE), secondary electrons (SE), scanning transmission electron microscopy (STEM), and secondary ion imaging (SI), with accelerating voltages of 0.2–30 kV. The maximum spatial resolution of the Helios NanoLab 650 was 1.1 nm at 15 kV.

Quantitative EDS microanalyses were performed on a JEOL JSM-5800 SEM at 20 kV. Spectra were acquired for 100 s at a detector dead time of 25–30 % and quantified using mineral standards recalculated to oxides. Calibration was regularly checked against a cobalt standard.

WDS analyses were conducted with a CAMECA SX-100 electron microprobe and a JEOL JSM-840 SEM (SGIDS, Bratislava) at 15 kV, 20 nA. Spot analyses determined the chemistry of olivine, pyroxenes, plagioclase, apatite, kamacite, taenite, chromite, and troilite in the meteorite Jesenice. Elements analyzed included F, Na, Si, Al, Mg, Cl, K, Ca, Ti, Fe, Mn, Cr, Ni, and P, along with trace elements in apatite (Y, U, Sr, Ba, REEs, Th, Zn, and V). Calibration standards included LiF (F), albite (Na), orthoclase and wollastonite (Si), orthoclase (K), $Al2O_3$ (Al), NaCl (Cl), wollastonite (Ca), TiO_2 (Ti), fayalite (Fe), rhodonite (Mn), forsterite and MgO (Mg), metallic Cr (Cr), metallic Ni (Ni), apatite (P), UO_2 (U), barite (Ba, S), $CePO_4$ (Ce), $LaPO_4$(La), $NdPO_4$ (Nd), $SmPO_4$ (Sm), $EuPO_4$ (Eu), $GdPO_4$ (Gd), $TbPO_4$ (Tb), $DyPO_4$ (Dy), $HoPO_4$(Ho), $ErPO_4$ (Er), $TmPO_4$ (Tm), $YbPO_4$ (Yb), ThO_2 (Th), willemite (Zn), and metallic V (V).

TEM analyses were carried out with JEOL JEM-2010F, JEM-ARM200F, and JEM-2100 instruments at 200 kV. TEM foils were prepared from selected regions of the meteorite Jesenice. Techniques included high-resolution TEM (HR-TEM), selected area electron diffraction (SAED), STEM, EDS, and bright-/dark-field imaging. The highest resolution (JEM-ARM200F, Sabanci University) was 0.08 nm. SAED patterns were indexed against the Inorganic Crystal Structure Database (ICSD).

Results

Petrography and mineral chemistry of shock veins

Optical analysis revealed the presence of 1–2 shock veins per thin section, each measuring approximately 5 × 10 mm. The shock veins in meteorite Jesenice are up to 1500 μm long and up to 30 μm thick (Fig. 2a). The distribution of the phases present in the shock veins is heterogeneous. Shock veins consist of metallic taenite (FeNi)/troilite (FeS) globules, nanocrystalline silicate melt,

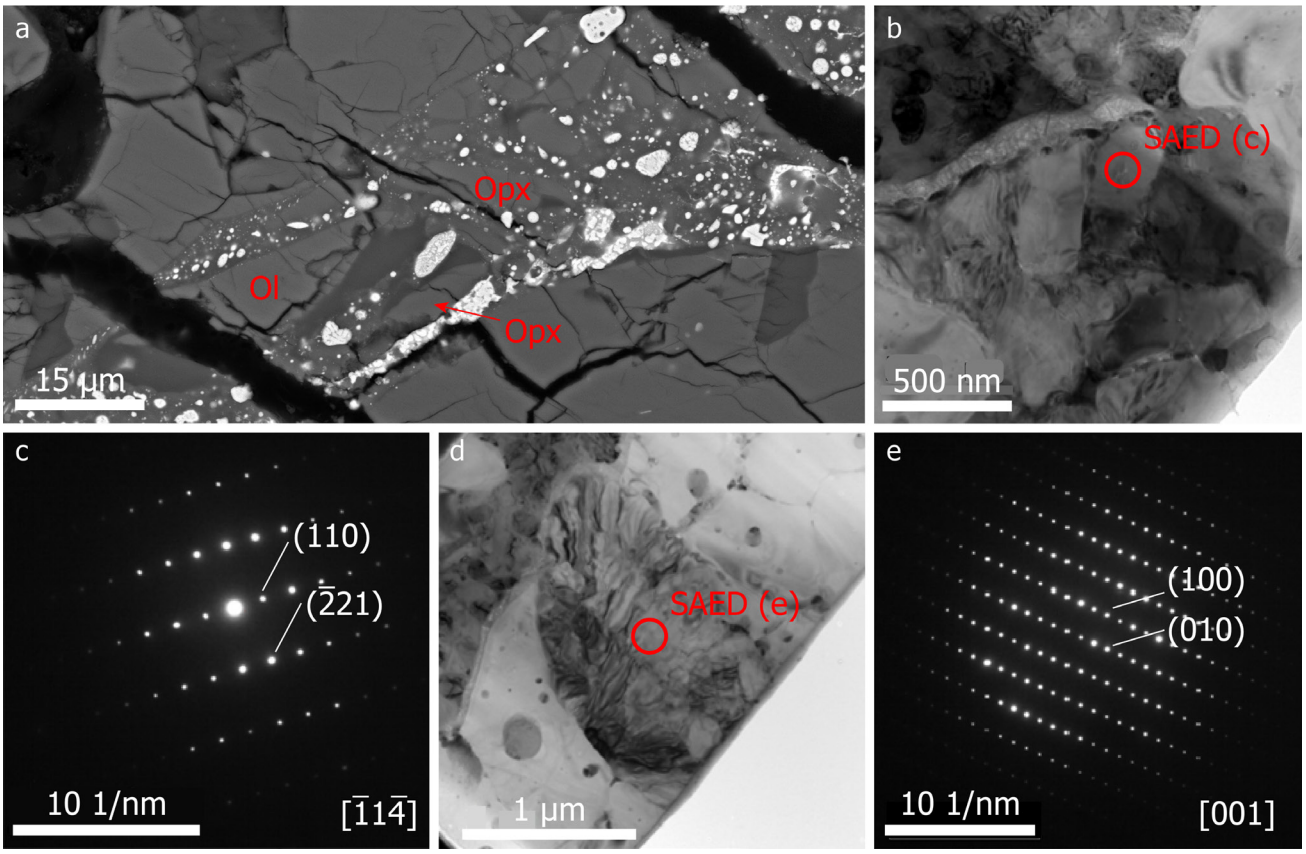

Fig. 2. Silicates in shock vein: (a) SEM image of a shock vein with marked silicate fragments (Opx – orthopyroxene, Ol – olivine); (b) TEM image of Opx; (c) SAED pattern of Opx; (d) TEM image of an olivine grain with a large number of dislocations; (e) SAED pattern of olivine.

and large fragments of silicate minerals. Metallic globules, together with the silicate melt occupy a thicker central part of the shock veins.

Fragments of silicate minerals in shock veins are mostly grains of olivine and orthopyroxene (Fig. 2b,c), with grain diameters ranging from 5 to 30 µm. The analyzed olivines are very homogeneous and predominantly forsteritic (Fo_{74-75}) (Table 1). Orthopyroxenes have enstatite compositions, with X_{Ca} = 0.01, X_{Mg} = 0.77, and X_{Fe} = 0.21. Transmission electron microscopy analysis of the olivine grains showed the presence of a large concentration of dislocations (Fig. 2d,e). However, the simultaneous shock and shear were sufficient to cause these grains to be pulled out of their original position and moved (possibly a few tens of microns to a few millimeters) along the shock vein.

Around large silicate grains, smaller metal-sulfide globules and submicrometer- to nanocrystalline silicate grains were found. Smaller metal-sulfide globules are usually scattered around these grains. Submicrometer-sized silicate grains are usually orthopyroxene, which acts as cement. The size of these grains ranges from 0.5–1 µm. Between the orthopyroxene grains, a cluster of 50 nm rounded olivine grains was observed. Round troilite blebs of 10–500 nm in size (similar to metallic globules) are also present (Fig. 2a).

Globules

Many different types of FeNi/FeS globules occur in the meteorite Jesenice (Fig. 3), which occupy about 50 vol.% of the shock veins. SEM analyses revealed the presence of four different types of FeNi/FeS globules (Fig. 3). The first type is globules of FeNi/FeS intergrowth (Fig. 3b), which are the largest type of globules that were found in the shock veins of the meteorite Jesenice. They occur in two different sizes: 3–15 µm and 100–200 nm. These globules form an almost perfect spherical shape. Some globules are elongated, possibly in the direction of flow (Fig. 3e–f). Secondary dendrites, reported in many other different chondrites (Scott, 1982), are not present. The average width of dendritic elongated FeNi cells is 0.1–1 µm. The second type are globules with dendritic/cellular structure (Fig. 3c), which are rare in this meteorite. The third type are irregular globules (Fig. 3d), which are common and can be up to several 10 µm in size. They have a similar internal composition to other types of globules but differ in their irregular shape, which merges with the silicate matrix of the shock vein. The fourth type is deformed globules (Fig. 3e), which were deformed by the shock process and indicate the direction of the melt flow.

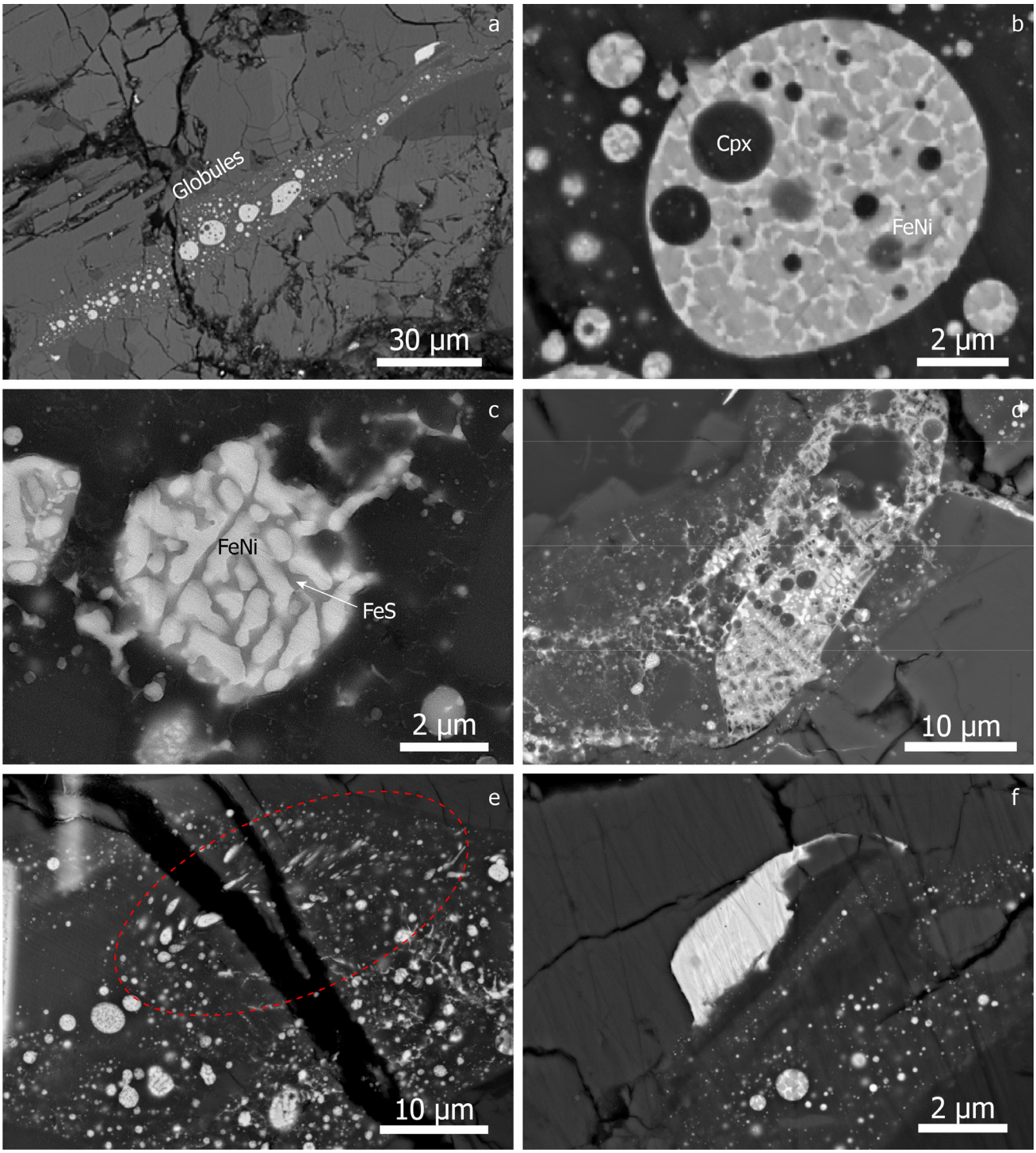

Fig. 3. SEM images of globules in shock veins in the meteorite Jesenice: (a) shock vein in the meteorite with globules; (b) globules of FeNi/FeS intergrowth; (c) globules with dendritic/cellular structure; (d) irregular globules; (e) elongated, oval-shaped globule (delineated by a dashed line); (f) heavily deformed FeNi mineral at the edge of the shock vein.

Globules of FeNi/FeS intergrowth were studied in detail with high-angle annular dark-field (HAADF) scanning transmission electron microscopy (STEM) analysis, which revealed a complex internal structure (Fig. 4). The main part of the globule consists of the eutectic intergrowth of FeNi/FeS minerals (Fig. 4a–c). Selected area electron diffraction (SAED) analysis revealed that all minerals occur in the same crystallographic orientation. Within the main globule many smaller, 1–2 µm sized, spherical subglobules occur (Fig. 4a). EDS analysis (Fig. 4d–f) showed that they consist of clinopyroxene with diopsidic composition (X_{Ca} = 0.45, X_{Mg} = 0.47, and X_{Fe} = 0.08), completely different from the orthopyroxenes found outside the shock veins in the host rock. Within the pyroxene subglobules, many smaller (10–200 nm) troilite blebs with the same crystallographic orientation are found. The main globule is surrounded by a 50–100 nm thick rim (Fig. 4g),

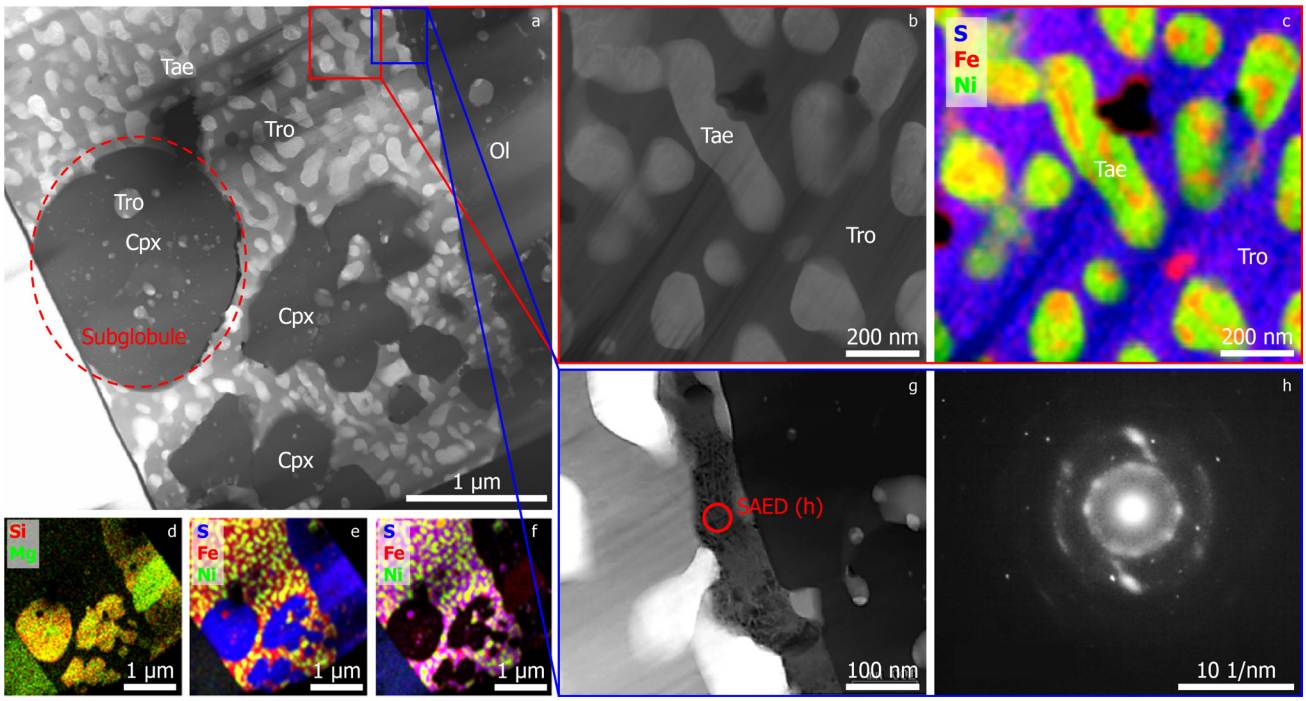

Fig. 4. STEM analysis of structures inside of FeNi/FeS globule: (a) HAADF-STEM image of a cross-section of the globule (Tae – taenite, Tro – troilite, Ol – olivine, Cpx – clinopyroxene); (b) detail of taenite/troilite intergrowth; (c) EDS map of taenite/troilite intergrowth; (d–f) EDS maps of a FeNi/FeS globule; (g) detail of globule rim; (h) SAED pattern of globule rim marked on figure g.

which consists of partially crystallized grains of clinopyroxene, as indicated in the corresponding SAED pattern (Fig. 4h).

The cooling rate of FeNi/FeS globules

To estimate cooling rates based on solid-state dendritic microstructures in the metallic phase for pre-shock or parent-body cooling, we used an equation proposed by (Scott, 1982):

$$R = 5.3 \ 10^5 d^{-2.9}$$

where R is cooling rate in Ks^{-1} and d is diameter of the dendrites (or in our case the width of the elongated cells in micrometers, as noted by (Blau & Goldstein, 1975), we estimated the cooling rate at $5.3 \cdot 10^5$ Ks^{-1} – $4.2 \cdot 10^8$ Ks^{-1}.

From the size of the globules observed in the meteorite Jesenice we have estimated the post-shock cooling rate, using the equation for a crystallizing melt sphere (Tsuchiyama et al., 1980):

$$R = \frac{3\varepsilon\sigma}{rp\left(C_p + \frac{\Delta H_c}{\Delta T_c}\right)} \left(T^4 - T_a^4\right)$$

where R is cooling rate (Ks^{-1}), σ is Stefan-Boltzmann constant (5.704×10^{-12} $Jcm^{-2}s^{-1}K^{-1}$), ε is emissivity, C_p is specific heat ($Jg^{-1}K^{-1}$), ΔH_c is enthalpy of crystallization (Jg^{-1}), ΔT_c is temperature interval of crystallization (K), T_a is ambient temperature (K), ρ = density (gcm^{-3}), and r is radius of the sphere (in this case FeNi/FeS globules) (cm).

We have used the following parameters, which have been adopted from (D'orazio et al., 2009): ε = 0.28 (emissivity of molten iron), C_p = 0.66 $Jg^{-1}K^{-1}$ (average Cp for FeS and FeNi at 1400 K), ΔH_c = 298 Jg^{-1} (average ΔHc for FeS and FeNi at 1400 K), (cooling from 1623 K to 1223 K), T_a = 200 K, ρ = 6.12 gcm^{-3} and r_1 = 0.5 µm in r_2 = 15 µm (minimum and maximum diameter of globules present in the meteorite Jesenice). The calculations show a cooling rate of $2.2 \cdot 10^5$ Ks^{-1} – $7.4 \cdot 10^3$ Ks^{-1}.

Discussion

The presence of shock veins filled with FeNi/FeS metal-troilite intergrowth grains indicate that shock veins formed by shock-induced melting followed by rapid quenching. Rounded olivine grains, together with a high frequency of dislocations, indicate that the olivine was severely damaged during the shock. For this reason, we have considered the melting temperature of olivine at a given shock pressure as the highest possible temperature during shock metamorphism. On the other hand, the chemical composition of clinopyroxenes in melt veins and the host rock is significantly different, implying the crystallization of clinopyroxenes in veins from the melt during shock metamorphism. Therefore, we propose the crystallization temperature of pyroxene as the lowest possible temperature during shock metamorphism. TEM analyses have shown that FeNi/FeS minerals and clinopyroxene present in globules crystallized from melt and

olivine did not melt during shock. This indicates that the peak temperature of shock metamorphism is 1500–2150 °C (Gasparik, 2014). Clinopyroxenes in globules are enriched with FeO compared to clinopyroxenes in the matrix and chondrules, which implies oxidation of the meteorite Jesenice parent body during the impact (Chen et al., 2002). The presence of olivine and Ca-pyroxene and the absence of plagioclase in the shock veins indicate shock pressures of 2.5–15 GPa (Agee et al., 1995). This is in agreement with the previously reported (Bischoff et al., 2011) classification of the meteorite Jesenice as an S3 chondrite. Our calculations showed a rapid after-shock cooling rate of $2.2 \cdot 10^5$ Ks^{-1} – $7.4 \cdot 103$ Ks^{-1}.

Our study showed that taenite in the globules is not surrounded by kamacite, which has been frequently reported in similar systems (Scott, 1982). This can be explained by the still ongoing thermal metamorphosis inside the meteorite Jesenice's parent body (Scott, 1982) after the shock metamorphic event had occurred for a limited time. The absence of kamacite around taenite in the globules is most readily explained if parent-body thermal metamorphism continued after the shock event; this scenario would imply that the impact preceded a period of longer-duration heating, although additional chronological or thermal-history data are required to confirm this sequence. Troilite inclusions in silicates in globules indicate exsolution of troilite during the shock. FeNi/FeS globules are a consequence of the immiscibility of metal-sulfide melt and silicate melt (Chen et al., 2002).

The oval shape of some globules could indicate the shear direction and that melting by a shear-friction mechanism, as noted by Xie et al. (2011), is the main reason for the formation of shock veins in the meteorite Jesenice and that crystallization took place during the shock.

We identified an ordered FeNi phase (tetrataenite) in the meteorite matrix (Fig. 5) with an approximately stoichiometric composition of 50 at.% Ni and 50 at.% Fe. The chemical composition of tetrataenite typically ranges from 46 to 56 at.% Ni (Clarke & Scott, 1980), in agreement with the values observed in the meteorite Jesenice (42–50 at.% Ni). The presence of tetrataenite in the matrix indicates that this ordered FeNi phase most likely formed after the shock event, under low-temperature and slow-cooling conditions, and was therefore not affected by shock. Together with the absence of kamacite in FeNi globules—which suggests that thermal metamorphism continued after the shock but before disruption of the parent body—the occurrence of tetrataenite further supports the interpretation that extended parent-body metamorphism followed the shock event. Our analyses indicate that the meteorite Jesenice cooled from the peak temperature of thermal metamorphism at a slow cooling rate of 1–100 K/Ma. The presence of tetrataenite supports this interpretation, as it is known to form only in slow-cooled meteorites (Clarke & Scott, 1980), further implying that meteorite Jesenice originated deep within its parent body (Wittmann et al., 2010). To constrain its thermal history, we applied two complementary approaches, each addressing different processes. First, we estimated cooling rates from the solid-state FeNi dendritic microstructures in the metallic phase (Scott, 1982), reflecting the long-term cooling within the parent body prior to any shock events. This provides insight into the slow thermal evolution in a deep, insulated environment. Second, we estimated the cooling rates of FeNi/FeS globules formed during the shock event, accounting for heat loss from individual molten globules, their size, latent heat of crystallization, and radiative cooling (Tsuchiyama et al., 1980).

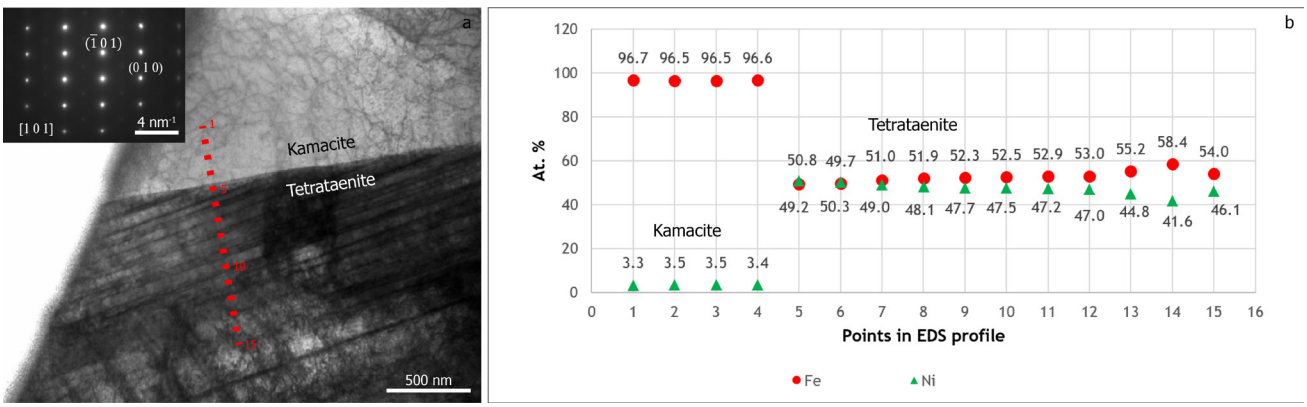

Fig. 5. TEM analysis of tetrataenite in meteorite Jesenice: (a) STEM image of kamacite – tetrataenite grain boundary with SAED pattern of tetrataenite in [1 0 1] (ICSD = 103556); (b) EDS profile of kamacite – tetrataenite grain boundary. The chemical composition of tetrataenite varies between 42 and 50 at.% of Ni.

This yields a realistic estimate of post-shock melt solidification, which occurs over a much shorter timescale than parent-body cooling. Together, these methods allow us to distinguish between slow pre-shock cooling and rapid post-shock solidification, providing a more complete picture of the thermal history of the meteorite Jesenice. Some parts of the shock veins show a partially melted transition zone, indicating that the shock melting took place *in situ*.

Conclusions

The presence of shock veins in the meteorite Jesenice indicates that the shock event was violent enough to cause partial melting of the meteorite. The presence of oval-shaped globules indicates the formation of shock veins as a consequence of shear friction melting. Peak pressure and temperature during shock were 2.5–15 GPa and 1500–2150 °C, respectively. The presence of tetrataenite in the meteorite Jesenice indicates, that the FeNi metal experienced slow cooling at temperatures below ~320 °C (Wasilewski, 1988), reflecting the low-temperature thermal history within the parent body, but it does not directly constrain the timing or location of the shock event.

Meteorite Jesenice is a good example of a weakly shocked chondrite, which provides the evidence for the hypothesis that local melting is not a result of severe shock, but a consequence of very locally increased pressure and temperature, most likely due to the shear-fracture mechanism, during shock.

Acknowledgments

We are thankful to the curator of the Slovenian museum of Natural History Miha Jeršek for providing samples of the meteorite Jesenice. This work was financially supported by the Slovenian Research and Innovation Agency (ARIS): Research Core Funding Nos. P2-0084 and P1-0195.

References

Acosta-Maeda, T.E., Scott, E.R.D., Sharma, S.K. & Misra, A.K. 2013: The pressures and temperatures of meteorite impact: Evidence from micro-Raman mapping of mineral phases in the strongly shocked Taiban ordinary chondrite. American Mineralogist, 98/5–6: 859–869. https://doi.org/10.2138/am.2013.4300

Agee, C.B., Li, J., Shannon, M.C. & Circone, S. 1995: Pressure–temperature phase diagram for the Allende meteorite. Journal of Geophysical Research, 100: 17725–17740.

Bischoff, A., Jeršek, M., Grau, T., Mirtič, B., Ott, U., Kučera, J., Horstmann, M., Laubenstein, M., Herrmann, S., Řanda, Z., Weber, M. & Heusser, G. 2011: Jesenice – A new meteorite fall from Slovenia. Meteoritics and Planetary Science, 46/6: 793–804. https://doi.org/10.1111/j.1945-5100.2011.01191.x

Blau, P.J. & Goldstein, J.I. 1975: Investigation and simulation of metallic spherules from lunar soils. Geochimica et Cosmochimica Acta, 39/3: 307–324. https://doi.org/10.1016/0016-7037(75)90199-4

Chen, M., Xie, X., Wang, D. & Wang, S. 2002: Metal-troilite-magnetite assemblage in shock veins of Sixiangkou meteorite. Geochimica et Cosmochimica Acta, 66/17: 3143–3149. https://doi.org/10.1016/S0016-7037(02)00903-1

Clarke, R.S. & Scott, E.R.D. 1980: Tetrataenite-ordered FeNi, a new mineral in meteorites. American Mineralogist, 65/1959: 624–630.

Gasparik, T. 2014: Phase Diagrams for Geoscientists. An Atlas of the Earth's Interior. Springer, New York: 462 p.

Guo, Z., Li, Y., Liu, S., Xu, H., Xie, Z., Li, S., Li, X., Lin, Y., Coulson, I.M. & Zhang, M. 2020: Discovery of nanophase iron particles and high pressure clinoenstatite in a heavily shocked ordinary chondrite: Implications for the decomposition of pyroxene. Geochimica et Cosmochimica Acta, 272: 276–286. https://doi.org/10.1016/j.gca.2019.10.036

Kong, P. & Xie, X. 2003: Redistribution of elements in the heavily shocked Yanzhuang chondrite. Meteoritics and Planetary Science, 38/5: 739–746. https://doi.org/10.1111/j.1945-5100.2003.tb00038.x

Owocki, K. & Muszyński, A. 2012: Shock veins in the Sahara 02500 ordinary chondrite. Geologos, 18/2: 111–118. https://doi.org/10.2478/v10118-012-0006-0

Robie, R., Hemingway, B. & Fisher, J. 1978: Thermodynamic properties of minerals and related substances at 298.15 K and 1 bar (105 pascals) pressure and at higher temperatures (Report No. 1452), Bulletin. https://doi.org/10.3133/b1452

Scott, E.R.D. 1982: Origin of rapidly solidified metal-troilite grains in chondrites and iron meteorites. Geochimica et Cosmochimica Acta, 46/5: 813–823. https://doi.org/10.1016/0016-7037(82)90032-1

Stoffler, D., Keil, K. & Scott, E.R.D. 1992: Shock Classication of Ordinary Chondrites: New Data and Interpretations. Meteoritics, 27/3: 292. http://ads.nao.ac.jp/cgi-bin/nph-bib_

query?bibcode=1992Metic..27R.292S&db_key=AST

Tsuchiyama, A., Nagahara, H. & Kushiro, I. 1980: Experimental reproduction of textures of chondrules. Earth and Planetary Science Letters, 48/1: 155–165. https://doi.org/10.1016/0012-821X(80)90178-8

Wasilewski, P.J. 1988: Magnetic characterization of the new magnetic mineral tetrataenite and its contrast with isochemical taenite. Physics of the Earth and Planetary Interiors, 52: 150–158. https://doi.org/10.1016/0031-9201(88)90063-5

Wittmann, A., Swindle, T.D., Cheek, L.C., Frank, E.A. & Kring, D. A. 2010: Impact cratering on the H chondrite parent asteroid. Journal of Geophysical Research: Planets, 115/7: E07009. https://doi.org/10.1029/2009JE003433

Xie, X., Sun, Z. & Chen, M. 2011: The distinct morphological and petrological features of shock melt veins in the Suizhou L6 chondrite. Meteoritics and Planetary Science, 46/3: 459–469. https://doi.org/10.1111/j.1945-5100.2011.01168.x

Xie, Z., Sharp, T.G. & De Carli, P.S. 2006: Estimating shock pressures based on high-pressure minerals in shock-induced melt veins of L chondrites. Meteoritics and Planetary Science, 41/12: 1883–1898. https://doi.org/10.1111/j.1945-5100.2006.tb00458.x